Photochemistry and Photobiology, 20**, **: *–*

Special Issue Research Article

Substituent and Surfactant Effects on the Photochemical Reaction of Some Aryl Benzoates in Micellar Green Environment†

Gastón Siano[1,2], Stefano Crespi[3] and Sergio M. Bonesi[1,2]*

[1]Departamento de Química Orgánica, Facultad de Ciencias Exactas y Naturales, Universidad de Buenos Aires, Buenos Aires, Argentina
[2]Centro de Investigaciones en Hidratos de Carbono (CIHIDECAR), CONICET–Universidad de Buenos Aires, Buenos Aires, Argentina
[3]Stratingh Institute for Chemistry, University of Groningen, Groningen, The Netherlands

Received 7 March 2021, accepted 9 April 2021, DOI: 10.1111/php.13431

ABSTRACT

In this study, we carried out preparative and mechanistic studies on the photochemical reaction of a series of p-substituted phenyl benzoates in confined and sustainable micellar environment. The aim of this work is mainly focused to show whether the nature of the surfactant (ionic or nonionic) leads to noticeable selectivity in the photoproduct formation and whether the electronic effects of the substituents affect the chemical yields and the rate of formation of the 5-substituted-2-hydroxybenzophenone derivatives. Application of the Hammett linear free energy relationship (LFER) on the rate of formation of benzophenone derivatives, on the lower energy band of the UV-visible absorption spectra of the aryl benzoates and 5-substituted-2-hydroxybenzophenone derivatives allows a satisfactory quantification of the substituent effects. Furthermore, UV-visible and 2D-NMR (NOESY) spectroscopies have been employed to measure the binding constant K_b and the location of the aryl benzoates within the hydrophobic core of the micelle. Finally, TD-DFT calculations have been carried out to estimate the energies of the absorption bands of p-substituted phenyl benzoates and 5-substituted-2-hydroxybenzophenone derivatives providing good linear correlation with those values measured experimentally.

INTRODUCTION

Designing photochemical reactions aiming to control the product selectivity represents a great challenge in synthetic organic photochemistry (1,2), especially when radical pairs or radical–ion pairs are formed as primary intermediates (3,4). Performing the photoreactions in water-soluble confined assemblies such as zeolites (5,6), micelles (7,8), polyolefin films (9), cavitands (10,11), or dendrimers (12) affords an intriguing control in the product distribution, because these confined assemblies impart a restricted mobility on the reactive intermediates generated after excitation. In particular, cationic, anionic and neutral surfactant micelles are confined assemblies that are capable of solubilizing in water hydrophobic molecules, *that is,* organic molecules. Furthermore, they have the ability to: (1) concentrate guest molecules into relatively small effective volumes (7,13), (2) exist in a dynamic equilibrium and (3) are capable to organize organic substrates (14,15). The control of the reactivity of radical species generated within the micelle and some physical parameters involved in their reactivity have been previously studied (14,15).

The hydrophobic cores in micelles can be considered as a microreactor where (photo)reactions can take place and can be helpful to direct the selectivity of the (photo)products. Likewise, the nature of the surfactant or the counterion effect is a notable feature that can affect the course of a photoreaction, modifying significantly the rate of formation of the photoproducts and perhaps, has influence on the overall chemical and quantum yields. A striking example is the effect of the nature of the surfactants on the photochemical reaction of p-benzoquinone and duroquinone. Anionic surfactants like sodium laurate and SDS accelerate the photoreaction, the nonionic Tween 80 shows no effect, and cationic surfactants such as CTAB markedly suppressed the photoreaction (16). The photoinduced reduction of β-arylquinone sulfates was markedly affected by when the photoreaction was carried out in water containing cationic surfactants (17). The tetra-*O*-acyl riboflavin photosensitized monomerization of thymine cyclobutane dimers benefited from the presence of cationic surfactants, whereas neutral and anionic surfactants inhibited the photosensitized reaction (18). The absorbance and fluorescence spectra of chloroquine were used to probe the effect of the counterions present in different cationic and anionic surfactants. While the nature of the counterion showed little effect on the chloroquine–micelle interaction, further evidence revealed that the interaction depends on the micellar surface charge (19).

Among the vast number of photochemical transformations, the photo-Fries rearrangement reaction represents a prototypical example to probe the micellar hydrophobic environment, counterion and substrate substituent effects. This photochemical reaction was discovered by Anderson and Reese (20), and it involves

*Corresponding author email: smbonesi@qo.fcen.uba.ar (Sergio M. Bonesi)
†This article is part of a Special Issue celebrating the career of Dr. Edward Clennan.

a homolytic cleavage of a carbon–heteroatom bond, *that is*, C-O, C-S and C-N (21,22), Hence, the photochemical reaction undergoes an in-cage radical mechanism. It is well-established that the reaction proceeds mainly through the singlet state (9,22), Scheme 1 depicts the photochemical reaction of (hetero)aryl benzoates displaying the *ortho*- and *para*-rearranged photoproducts as well as the corresponding phenol (21).

The competition between in-cage radical recombination versus out-of-cage diffusion dictates the product distribution of the photo-Fries rearrangement reaction. The characteristics of the environment influence the choice between these two paths, and consequently aryl esters are ideal candidates to study micellar environments (23–25). Indeed, the photo-Fries reaction of benzamides is documented in sodium dodecyl sulfate (SDS) micellar solution (26). Also, the photorearrangement of a variety of substituted acetanilides showed high selectivity in favor of the 5-substituted-2-aminoacetophenones in micellar solution (27). Furthermore, cyclodextrines as confined environments was found to influence the product distribution of the photo-Fries rearrangement of acetanilides (28) and phenyl esters and phenyl amides, respectively (29).

The preparation of benzophenone derivatives is an elegant example of the application of photochemistry in organic synthesis. Benzoyloxy benzophenones and their derivatives have demonstrated biological activity and pharmaceutical properties such as estrogenic activity and anti-inflammatory property, and their preparation involves the use of benzophenones as key synthons (30–33). Therefore, we performed a systematic study of the photo-Fries rearrangement of a series of *p*-substituted phenyl benzoates in micellar solution in order to evaluate: (1) the effect of the nature of the surfactant, viz. cationic, anionic or neutral surfactants on the consumption of the aryl benzoates and the formation of the photoproducts, (2) the effect of the substituents at *para*-position of the benzoates on the photoreaction and, (3) the constrained environment of the micelles to provide a high selectivity toward the formation of 5-substituted-2-hydroxy benzophenones. The structures of the aryl benzoates as well as the structures of the surfactants employed in this systematic study are shown in Scheme 2.

Herein, we describe the results obtained on the direct irradiation of several *para*-substituted aryl benzoates in confined and sustainable micellar solutions. From a preparative viewpoint, the photoreaction shows high selectivity toward the formation of 5-substituted-2-hydroxybenzophenone derivatives in good to excellent yields (higher than 90%). The location of the aryl benzoates within surfactant micelles (ionic and nonionic micelles) behaving as microreactors was demonstrated using NOESY NMR spectroscopy while the binding constant K_b of the substrates was measured by UV-visible spectroscopy.

MATERIALS AND METHODS

Materials. p-Chloro phenol, ethyl p-hydroxyphenylcarboxylate, benzoyl chloride, pyridine, sodium dodecyl sulfonate, cetyltrimethylammonium chloride and Brij-P35 were obtained from commercial sources. Aryl benzoates **1–6**, **9** and **10** and the corresponding benzophenone derivatives have been prepared according to the methodology reported previously in the literature (34). Spectroscopic grade solvents were used as received. Pyridine was distilled and stored over KOH pellets. Melting points were determined with a Fisher-Johns apparatus and are not corrected. ^{1}H and ^{13}C NMR spectra were recorded in $CDCl_3$ on a 300 MHz spectrometer; chemical shifts (δ) are reported in parts per million (ppm), relative to signal of tetramethylsilane, used as internal standard. 2D NOESY spectra were recorded in D_2O on a 500 MHz spectrometer, using a NOESY-ph pulse sequence with a 600 ms mixing time and a recovery delay of 1.5 s. 2K data points were collected for 512 increments of 16 scans, using TPPI f1 quadrature detection; chemical shifts (δ) are reported in parts per million (ppm), relative to the signal of trimethylsilylpropionic acid, used as internal standard. Coupling constant (J) values are given in Hz. The measurements were carried out using standard pulse sequences. GC analysis was carried out on a Hewlett Packard 5890 gas chromatograph using an Ultra 2 capillary chromatographic column. The chromatograms were recorded with the following program: initial temperature: 100°C, 2 min; gradient rate: 10°C min^{-1}; final temperature: 250°C, 10 min. The UV-visible spectra were measured with a Shimadzu UV-1203 spectrophotometer using two-faced stoppered quartz cuvettes (1 mm × 1 mm) at 298 K.

Determination of the binding constants (K_b) of aryl benzoates in micellar media. Solutions of aryl benzoates were prepared in deionized water (MilliQ), and their concentration varied between $5.5{\cdot}10^{-5}$ M and $1.0{\cdot}10^{-4}$ M. An aliquot (2 mL) of the phenyl benzoate solution was placed in fluorescence stoppered quartz cuvette provided with a stirring bar, and the UV-visible spectrum was recorded. The initial absorbance value at the maximum absorption wavelength (A_0) was read. Subsequently, aliquots of concentrated surfactant solution (10 μL) were added. The A value at the maximum absorption wavelength for each solution was consequently recorded. After each addition of surfactant, the solution was stirred for 20 min before measuring the absorbance. With the values of A_0 and A in hands, the values of $(A_0/(A–A_0))$ versus the reciprocal of the concentration of the micellar surfactant were plotted and the data were fitted with a linear regression program. The K_b values were obtained calculating the ratio of the slope and the origin.

Synthesis of aryl benzoates 7 and 8. To a solution of the substituted phenols (0.010 mol) in pyridine (10 mL) cooled in an ice-bath, benzoyl chloride (0.012 mol) was added dropwise in 10 min under stirring. Subsequently, the reaction mixture was kept under stirring for 60 min. After total consumption of the starting material was confirmed by TLC, the reaction mixture was extracted with dichloromethane (10 mL) and washed with a solution of diluted HCl (10 mL). The organic phase was then washed with water, dried on Na_2SO_4, filtrated and evaporated under pressure. The phenyl benzoates were purified from the solid residue by recrystallization using ethanol–water mixtures giving the corresponding phenyl benzoates in excellent yields (>90%). The aryl benzoates **7** and **8** were characterized comparing the melting points (m.p.) and spectroscopic data (^{1}H-NMR and ^{13}C-NMR) with the ones reported in the literature (see Supporting Information).

Photoirradiations of aryl benzoates in cyclohexane. A stock solution of a given benzoate (**1–10**, 0.1 mmol in 200 mL cyclohexane) was placed in a stoppered Erlenmeyer quartz flask and degassed with argon

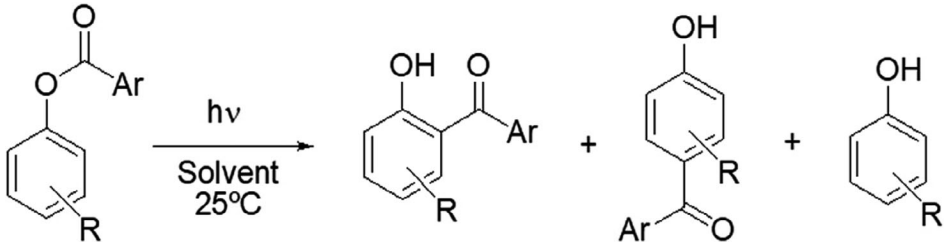

Scheme 1. The photo-Fries rearrangement of aryl benzoates.

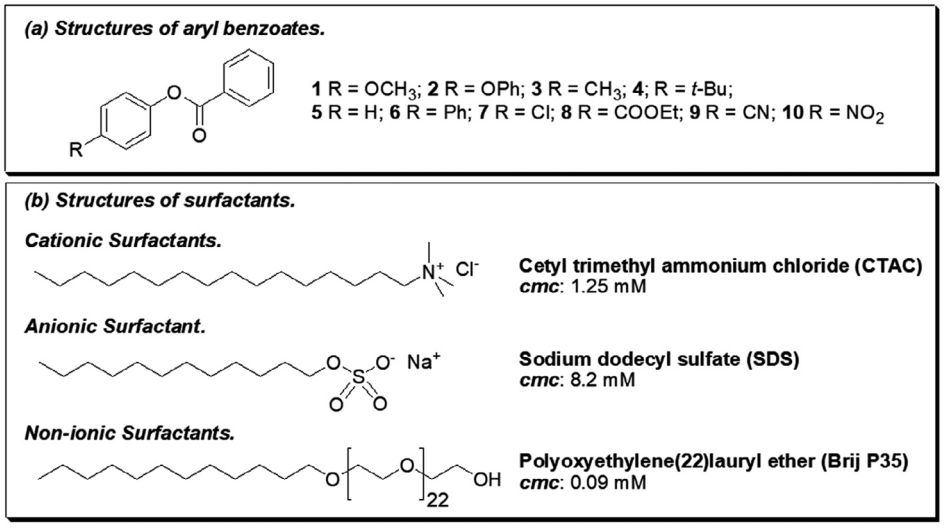

Scheme 2. Structures of the aryl benzoates and the surfactants studied.

for 30 min. The flask was placed in a homemade optical bench able to switch between a four or eight lamp irradiation setup. The solution was stirred during the entire irradiation. Irradiations with $\lambda_{exc} = 254$ nm were carried with four germicide lamps (Philips, each of 20 Watts). The reaction progress was monitored by TLC [eluent: hexane–ethyl acetate (8:2 v/v); spots were visualized with UV light (254 and 366 nm)] and by GC analysis (Ultra 2 capillary column, *vide supra*). When the conversion of the starting material was higher than 90%, the photolyzed solution was carefully evaporated to dryness under reduced pressure. The yellowish solid residue obtained was purified by silica gel column chromatography (eluent: hexane 100% followed by hexane–ethyl acetate mixtures). From the eluted fractions, the photoproducts were isolated and characterized by means of physical and spectroscopic methods.

Photoirradiations of aryl benzoates in micellar media. Stock solutions of surfactants in deionized water (SDS 0.10 M, CTAC 0.02 M and Brij-P35 0.05 M) were freshly prepared before each experiment. The aryl benzoate (5 mg) was placed in a stoppered quartz cell provided with a stirring bar (3 mL), and the surfactant stock solution (2 mL) was added. Then, the solution was vigorously stirred for one hour and degassed with argon for 20 min. The quartz cell was placed in a homemade optical bench provided with two germicide lamps (each of 20 W). The progress of the photoreaction was monitored by two different methods: (i) UV-visible spectroscopy and GC analysis (Ultra 2 capillary column). The conversion of the benzoates was kept below 20% to avoid secondary reactions and the formation of by-products. Previously to the injection into the GC apparatus, the micellar solutions were treated as follows. The photolyzed solutions were diluted with 2 mL of an aqueous solution of NaCl and then extracted with ethyl acetate (3×2 mL) while the system was carefully shaken to avoid the formation of emulsions. The organic layer was separated, dried over Na_2SO_4 and evaporated to dryness under vacuum. The yellowish solid residue was diluted in dichloromethane (2 mL), and this solution was injected into the GC for chromatographic analysis. The products were characterized by comparison with the ones reported in the literature (see Supporting Information).

Computational analysis. All the structures were prescreened using the CREST driver in the xTB software (35), using the GFN2-xTB level. In this way, the most stable conformers for each structure were picked via the default series of metadynamics and dynamics runs implemented in the driver, and reoptimized at the PW6B95D3/def2-SVP level, modeling the molecule in cyclohexane and methanol via the SMD implicit solvent method. The UV-vis spectra were calculated simulating the first 30 singlet transitions at the TD-PBE0/6-311 + g(2d,p)//PW6B95D3/def2-SVP and TD-CAM-B3LYP/6-311 + g(2d,p)//PW6B95D3/def2-SVP. All structures were confirmed to be minima by the absence of imaginary vibrational modes. All the DFT and TD-DFT calculations were carried out via Gaussian 16, Rev. B.01 (36).

RESULTS AND DISCUSSION

Photoirradiation of aryl benzoates in CTAC micellar media

In order to analyze if cationic, anionic and neutral micelles can function as photochemical microreactors and are able to induce photoproduct selectivity from aryl benzoates, the photo-Fries rearrangement reaction of a series of p-substituted phenyl benzoates was investigated in CTAC micellar media and was compared with those results that have been previously obtained (34). The general photochemical reaction of aryl benzoates is depicted in Scheme 3.

Irradiation of aryl benzoates (**1**–**10**) in CTAC micellar solutions with light of 254 nm under air provided 5-substituted-2-hydroxybenzophenone (**1a**–**10a**) with noticeable selectivity and in high yields (for structures, refer to Scheme 2). The photochemical reactions were carried out until 95% consumption of the aryl benzoates (**1**–**10**). The chemical yields of benzophenone derivatives (**1a**–**10a**) are collected in Table 1.

As is apparent from Table 1, the CTAC micro-heterogeneous media induced a high selectivity on the product distribution of the photoreaction, favoring the formation of benzophenone derivatives. The clean and high-yield (up to >99%) one-pot photo-Fries rearrangement of the aryl benzoates into 5-substituted-2-hydroxybenzophenones in micelles stands out as an efficient synthetic transformation. Indeed, phenolic and benzoic acid by-products were detected only to a minor extent or not detected at all in the micellar reaction mixture, while irradiation of aryl benzoates in cyclohexane provided a distinct product distribution (see Table 1), where the benzophenone derivatives were formed only in low yields. On the other hand, the high selectivity for the formation of benzophenone derivatives in CTAC micellar media (Table 1) is similar to the high selectivity obtained in SDS and Brij-P35 micellar solutions (34). Therefore, these results led to conclude that the selectivity and the high yield of benzophenone derivatives observed during the photochemical reaction of aryl benzoates under micellar condition seem to be unaffected by the nature of the surfactant, viz. anionic surfactant SDS, neutral surfactant Brij-P35 and cationic surfactant CTAC.

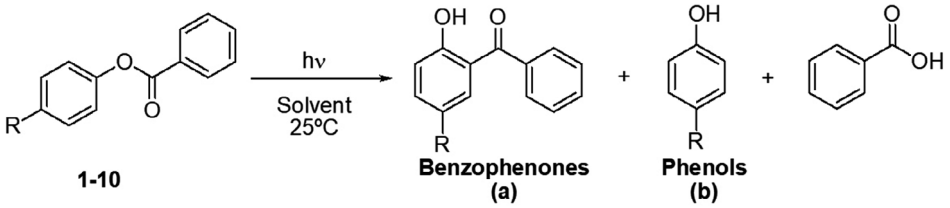

Scheme 3. The photochemical Fries rearrangement of aryl benzoates.

Table 1. Yields of photoproducts* and reaction quantum yield (ϕ_r)† measured in cyclohexane and CTAC micellar media.

	Photoproduct yields (%)			Reaction quantum yield (ϕ_r)	
	Cyclohexane‡		CTAC		
Aryl benzoates; R	Benzophenones (a)	Phenols (b)	Benzophenones (a)	Cyclohexane‡	CTAC
1; OMe	46	27	93	0.30	0.29
2; OPh	55	28	89	0.37	0.17
3; Me	42	22	88	0.40	0.14
4; t-Bu	59	27	87	0.50	0.27
5; H	40§	30	90¶	0.35	0.41
6; Ph	41	23	84	0.59	0.50
7; Cl	52	21	97	0.47	0.30
8; COOEt	48	24	>99	0.42	0.28
9; CN	38	19	>99	0.51	0.14
10; NO_2	31	34	54	0.02	0.05

*Yield of photoproducts determined by ^{1}H NMR spectroscopy in the reaction mixture. Concentration of aryl benzoates: 5.0×10^{-3} M. †Actinometer: KI (0.6 M), KIO_3 (0.1 M) and $Na_2B_2O_7{\cdot}10H_2O$ (0.01 M) solution in water; $\phi(I_3^-) = 0.74$; $\lambda_{exc} = 254$ nm.(37) Error: ± 0.01. ‡Data taken from Ref. (34). §4-Hydroxybenzophenone is also formed in 27%. ¶4-Hydroxybenzophenone is also formed in 8–10%.

Furthermore, this methodology gains relevance in organic synthesis because it is possible to carry out the photochemical reaction in aqueous solution with surfactants, despite of their charge. Also, this photochemical methodology shows a good tolerance of a wide variety of electron-donor and electron-acceptor groups attached to the aryl moiety of the aryl benzoates.

The observed selectivity toward the benzophenone derivatives over the corresponding phenols was attributed to the confinement of the esters and the radical species formed after the C-O bond cleavage within the micellar hydrophobic core. Furthermore, the micelle reduces the mobility of the primary radical species suppressing the formation of photoproducts that arise from the out-of-cage diffusion to the bulk solution.

The quantum yields of consumption of the aryl benzoates (ϕ_r) in CTAC solution and in cyclohexane are also collected in Table 1, showing comparable order of magnitude. However, the ϕ_r values measured in CTAC solutions were smaller than in cyclohexane. This distinct behavior accounts for a significant increase in the nonradiative and intersystem crossing pathways from the singlet excited state of aryl benzoates (**1–9**) in CTAC micellar solutions which competes efficiently with the photo-Fries rearrangement reaction pathway, whereas in cyclohexane such a competition was not observed. Additionally, it was found that the ϕ_r of aryl benzoates measured in CTAC solution are similar and in the same order of magnitude as it was obtained previously in SDS and Brij-P35 (34).

In the case of p-nitrophenyl benzoate (**10**), the ϕ_r values were found to be one order of magnitude lower than the other aryl benzoates in all the solvents studied. The spin-coupling effect of the nitro group attached at *para*-position of the phenyl moiety favors the intersystem crossing pathway. The fast nonradiative deactivation pathway of the singlet excited state competes efficiently with the photo-Fries rearrangement reaction (38,39). A similar behavior regarding the spin-coupling effect of the nitro group has been reported with nitro(hetero)arene derivatives (40,41).

Effect of the nature of the surfactants and the substituents on the photoreaction of aryl benzoates

UV-visible spectroscopy was used to follow the photochemical reaction of the aryl benzoates (**1–10**) in homogeneous (cyclohexane) and heterogeneous media (SDS 0.10 mol dm^{-3}, Brij-P35 0.10 mol dm^{-3} and CTAC 0.02 mol dm^{-3} solutions). The solutions of the aryl benzoates (5.0×10^{-5} mol dm^{-3}) were irradiated with light of 254 nm under inert atmosphere. For example, Fig. 1 shows the time-resolved UV-vis spectra of benzoates **1** and **3** in a micellar solution of CTAC 0.02 mol dm^{-3} where new absorption bands located at 374 nm and 350 nm for both benzoates grow-in with irradiation time. These new bands were assigned to the n,π* electronic transition of the carbonyl group of 2-hydroxybenzophenone derivatives **1a** and **3a**, respectively (38,39). Moreover, these new bands were also observed in the time-resolved UV-vis spectra of benzoates **1** and **3** recorded in cyclohexane as well as in SDS and Brij-P35 micellar solutions (see Figure S1). A similar spectroscopic behavior was also observed for all the other aryl benzoates (**2**, **4–10**) in all the solvents studied.

In order to analyze the solvent and the substituent effects on the UV-visible absorption spectra of the aryl benzoates (**1–10**) and 5-substituted-2-hydroxybenzophenones (**1a–10a**), the absorption spectra were recorded in homogeneous and micro-

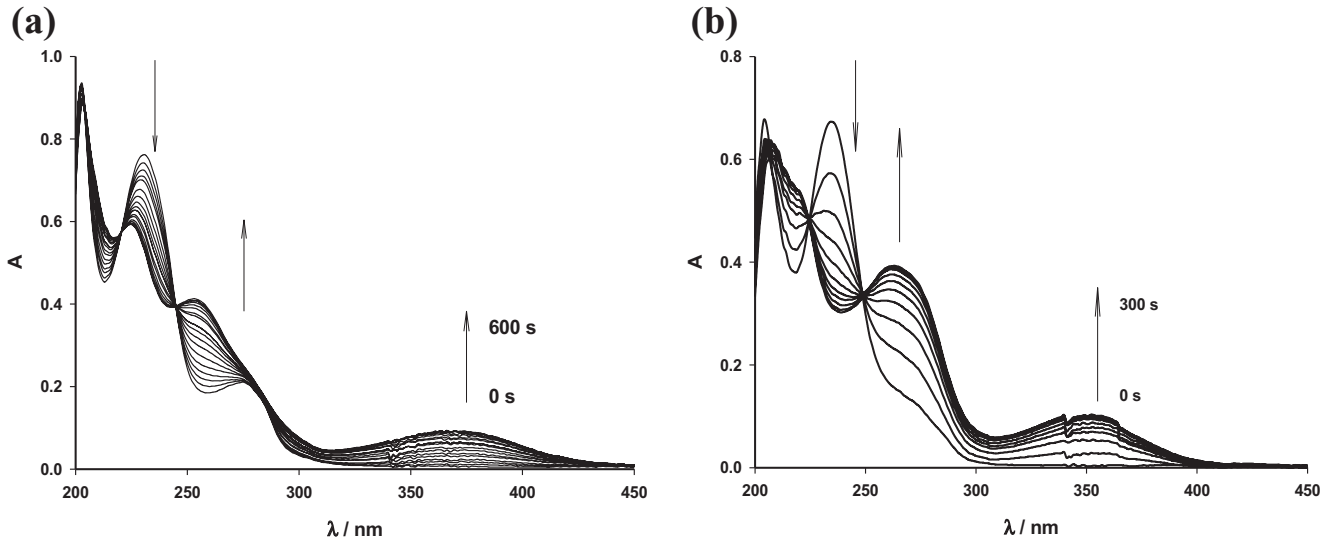

Figure 1. Time-resolved UV-visible absorption spectrum of (a) p-methoxyphenyl benzoate **1** and (b) p-methylphenyl benzoate **3** in solution of CTAC 0.02 mol dm^{-3}.

heterogeneous media. Table 2 collects the maximum absorption wavelengths (λ_{abs}) and the associated energy (E) values for the aryl benzoates and the corresponding benzophenone derivatives in cyclohexane, methanol and micellar solutions of SDS, Brij-P35 and CTAC.

Table 2 shows that there is no significant effect of the solvent on the maximum absorption wavelengths and hence on the energy values of the aryl benzoates as well as the 2-hydroxybenzophenone derivatives. Furthermore, no change of the λ_{abs} was observed when the hydrophobic core of the micelles as the solvent medium was compared with the data recorded in cyclohexane. However, a noticeable substituent effect was observed on the energy values of the aryl benzoates and the corresponding benzophenone derivatives (see Table 2), and this effect was quantified by means of the

Table 2. Energy (**E**) and maximum absorption wavelengths (λ_{abs}) values of the UV-visible lower energy band of aryl benzoates (**1**–**10**) and 5-substituted-2-hydroxybenzophenone (**1a**–**10a**) in different solvents.

	Cyclohexane		Methanol		SDS (0.10 M)		Brij (0.10 M)		CTAC (0.02 M)	
	λ_{abs} (nm)	E (ev)	λ_{abs} (nm)	E (ev)	λ_{abs} (nm)	E (ev)	λ_{abs} (nm)	E (ev)	λ_{abs} (nm)	E (ev)
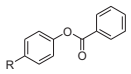										
OMe (**1**)	273	4.53	275	4.49	274	4.51	274	4.51	275	4.49
OPh (**2**)	269	4.59	272	4.54	272	4.54	272	4.54	274	4.51
Me (**3**)	266	4.64	270	4.57	273	4.53	272	4.54	271	4.53
t-Bu (**4**)	262	4.72	267	4.62	269	4.59	268	4.61	268	4.61
H (**5**)	266	4.64	258	4.79	263	4.70	268	4.61	264	4.68
Ph (**6**)	250	4.94	247	5.00	254	4.87	253	4.89	255	4.85
Cl (**7**)	231	5.35	233	5.30	236	5.24	238	5.19	235	5.26
COOEt (**8**)	238	5.19	239	5.18	243	5.09	240	5.15	241	5.13
CN (**9**)	238	5.19	238	5.19	240	5.15	239	5.17	241	5.13
NO_2 (**10**)	266	4.64	269	4.59	276	4.48	273	4.53	275	4.49
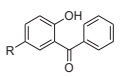										
OMe (**1a**)	375	3.30	374	3.30	373	3.31	372	3.32	374	3.30
OPh (**2a**)	357	3.46	357	3.46	357	3.46	360	3.43	352	3.51
Me (**3a**)	353	3.50	353	3.50	352	3.51	353	3.50	355	3.48
t-Bu (**4a**)	341	3.62	348	3.55	348	3.55	348	3.55	335	3.69
H (**5a**)	340	3.64	334	3.70	336	3.68	345	3.58	340	3.64
Ph (**6a**)	355	3.48	340	3.63	350	3.53	346	3.57	348	3.55
Cl (**7a**)	353	3.50	344	3.59	354	3.50	350	3.69	350	3.69
COOEt (**8a**)	330	3.74	323	3.82	329	3.76	332	3.73	325	3.80
CN (**9a**)	331	3.73	324	3.81	329	3.76	331	3.73	330	3.75
NO_2 (**10a**)	328	3.77	306	4.04	350	3.53	324	3.81	329	3.76

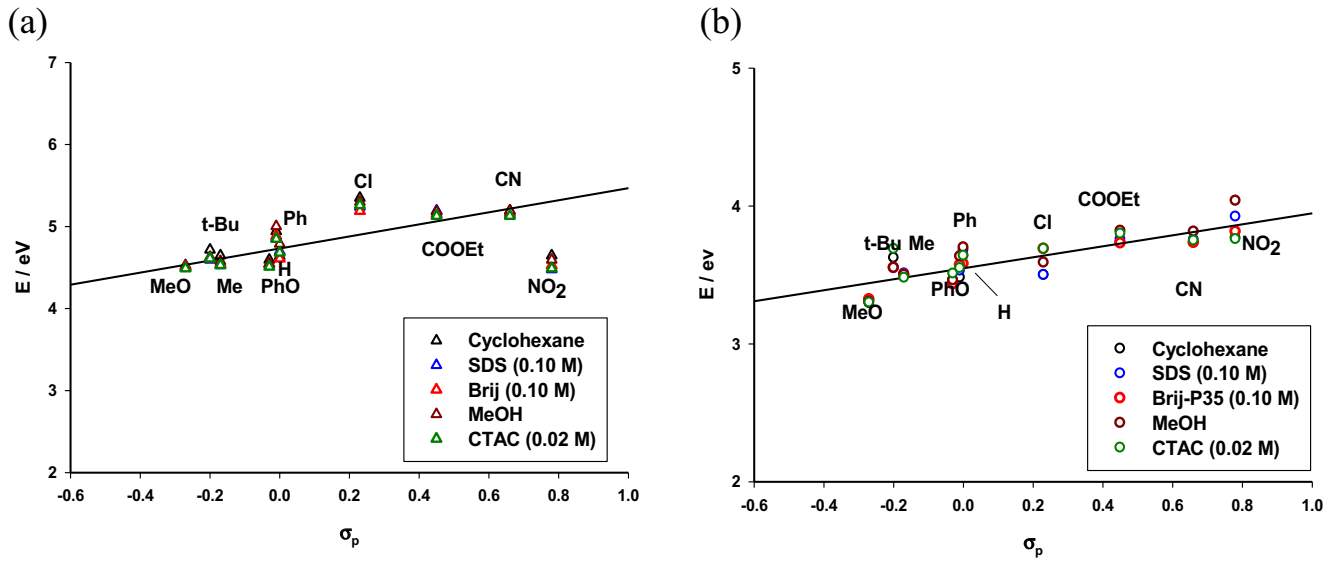

Figure 2. Hammett Correlation of the UV-visible lower Energy band (**E**) of (a) aryl benzoates and (b) 5-substituted-2-hydroxy-benzophenones in different solvents.

Hammett linear free energy relationships (LFER) (42,43). Thus, Eq. 1 describes the Hammett LFER where the energy values $E(R = X)$ at the maximum absorption wavelengths are correlated with Hammett substituent constants (σ_p) (44).

$$E(R=X) = r.s_p + E(R=H)$$

please change to

$$E(R=X) = \rho.\sigma_p + E(R=H) \quad (1)$$

The ρ value is a constant reflecting the sensitivity of the spectroscopic parameter values to the substituent and $E(R = H)$ is the energy value of the phenyl benzoate or 2-hydroxybenzophenone, respectively. Then, Fig. 2 shows the linear correlation fittings that were obtained with the σ_p Hammett parameters and the absorption energies (E) of substituted aryl benzoates and 2-hydroxybenzophenones by applying Eq. 1.

A nice linear correlation was obtained for the case of the aryl benzoates as can be seen in Fig. 2a displaying a slope ρ value of 0.70 ($r^2 = 0.90$) and an $E(R = H)$ value of 4.69 eV. Then, we can say that the energy of the absorption band under study is mostly affected by the electronic ability of the substituent itself in promoting hypsochromic shifts of the spectroscopic band. Indeed, the linear regression shows that as the electron-withdrawing character of the substituents increases, the absorption wavelength decreases noticeably. It is worth noticing that the linear regression was performed using the whole data obtained in all the solvents studied due to the absence of solvent effect. Likewise, Fig. 2b shows a good linear correlation for the family of 5-

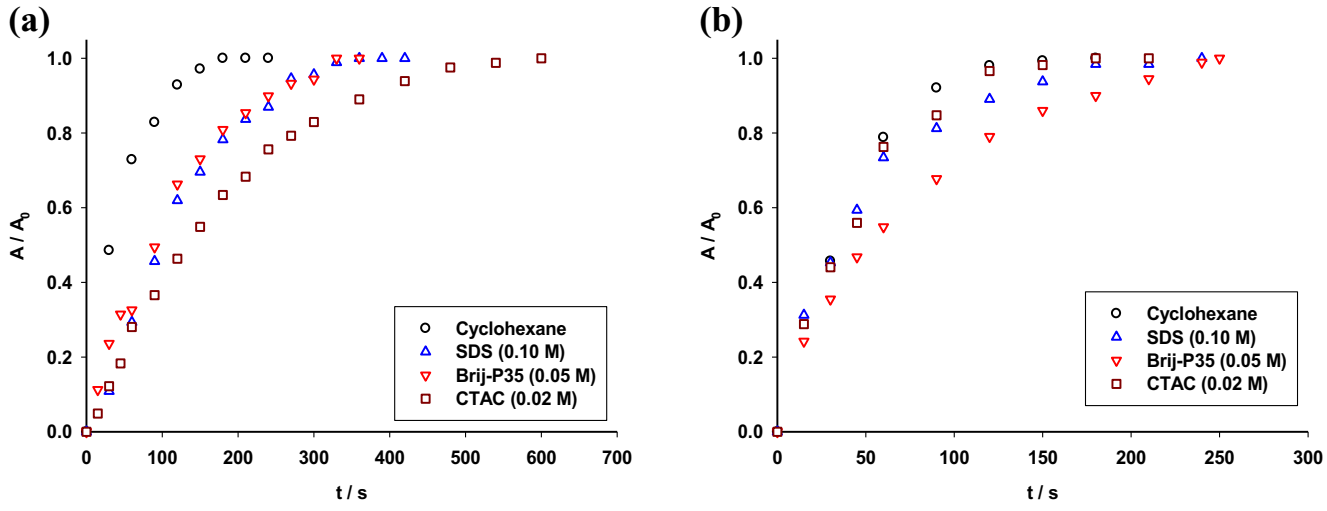

Figure 3. Relative absorbance (A/A_∞) of formation of: (a) benzophenone **1a** at 374 nm and (b) benzophenone **9a** at 331 nm, in cyclohexane and micellar solutions.

substituted-2-hydroxybenzophenones giving a slope ρ value of 0.40 ($r^2 = 0.91$) and an E(R = H) value of 3.54 eV. Therefore, a hypsochromic shift of the absorption wavelength was observed as the electron-withdrawing character of the substituents increases.

On the other hand, we have selected aryl benzoates **1** and **9** in order to analyze the solvent effect on the relative formation of 2-hydroxybenzophenones **1a** and **9a**, respectively, through the measuring of the relative absorption values (A/A_∞) as depicted in Fig. 3. The relative rates of formation of **1a** in surfactant media (see Fig. 3a) are slightly lower than in cyclohexane and radiative, and nonradiative decay rates account for the observed trend indicating a significant competition with the photoreaction pathway. Furthermore, the relative rate of compounds **1a** in CTAC solution is significantly lower than in SDS or Brij-P35 solutions attributing this behavior to the appreciable effect of the nature of the surfactant on the photoreaction. Indeed, CTAC is a tetraalkylammonium chloride and the chloride anion has the ability to quench the singlet excited state of the aryl benzoate promoting the deactivation through the intersystem crossing pathway. This quenching process became efficiently because the chloride anion operates like an external heavy atom quencher (38,39). A similar behavior was observed for the other aryl benzoates and the relative rates of formation (A/A_∞) of the corresponding benzophenones in cyclohexane and in different surfactant solutions are depicted in Figure S2.

However, for aryl benzoate **9** the relative absorbance (A/A∞) of formation of benzophenone **9a** in CTAC solutions shows a similar profile as in cyclohexane and SDS solution but are higher than in Brij-P35 solution. This peculiar behavior is due to an intramolecular quenching of the singlet excited state of benzoates **9** through a spin–orbit coupling process because this benzoate bears a cyano group which is a *pseudo*-halogen group. Therefore, no external heavy atom effect of the chloride anion on the benzophenone relative rates could be observed.

Next, we decided to study the effect of the substituents on the photochemical reaction of the aryl benzoates in micellar solution and in cyclohexane through the photoreaction rate constants (k). Once again, we applied the Hammett correlation to quantify effectively the substituent effect employing the linear regression depicted in Eq. 2,

$$\log(k/k_0) = \rho.\sigma_p \qquad (2)$$

where k represents the rate constants for p-substituted phenyl benzoates while k_0 represents the rate constant for phenyl benzoate. The rate constants (k) were easily gathered from the relative grow-in (A/A_0) of the benzophenones profiles shown in Fig. 4a for each p-substituted aryl benzoates (**1a**–**9a**) recorded in CTAC (0.02 M) aqueous solution. The same kinetic data were also raised involving a first order kinetic analysis for the consumption of each p-substituted aryl benzoates in micellar solution as well as in cyclohexane (see Figure S4). Then, with the rate constants measured in CTAC (0.02 M) aqueous solution in hand, a Hammett plot was constructed and a linear correlation was obtained providing a slope ρ of 0.69 and R-square of 0.836 (Fig. 4b). The substituent effect does not play an important role on the homolytic fragmentation of the C-O bond of the ester during the photo-Fries rearrangement reaction of the p-substituted phenyl benzoates as can be judged from the magnitude of the ρ value. Furthermore, the positive sign of ρ shows that as the electron-withdrawing character of the substituents increases, the rate constants increase noticeably. The electron-donor substituents have the opposite effect.

Linear regression on Hammett's plot was also obtained with the rate constants measured in micellar solutions (SDS 0.10 M and Brij-P35 0.10 M) and in cyclohexane providing a ρ value of 0.74 which is similar to that obtained for the CTAC solution (see Figure S5). This linear trend led to conclude that electron-withdrawing substituents increase whereas electron-donor substituents diminish the rate constants, as it was described previously in the case of the measurements performed in CTAC solution.

Location of the aryl benzoates in the micellar and measurement of the binding constants (K_b)

We applied 2D NMR (NOESY experiments) and UV-visible spectroscopies to estimate the location of the aryl benzoates and

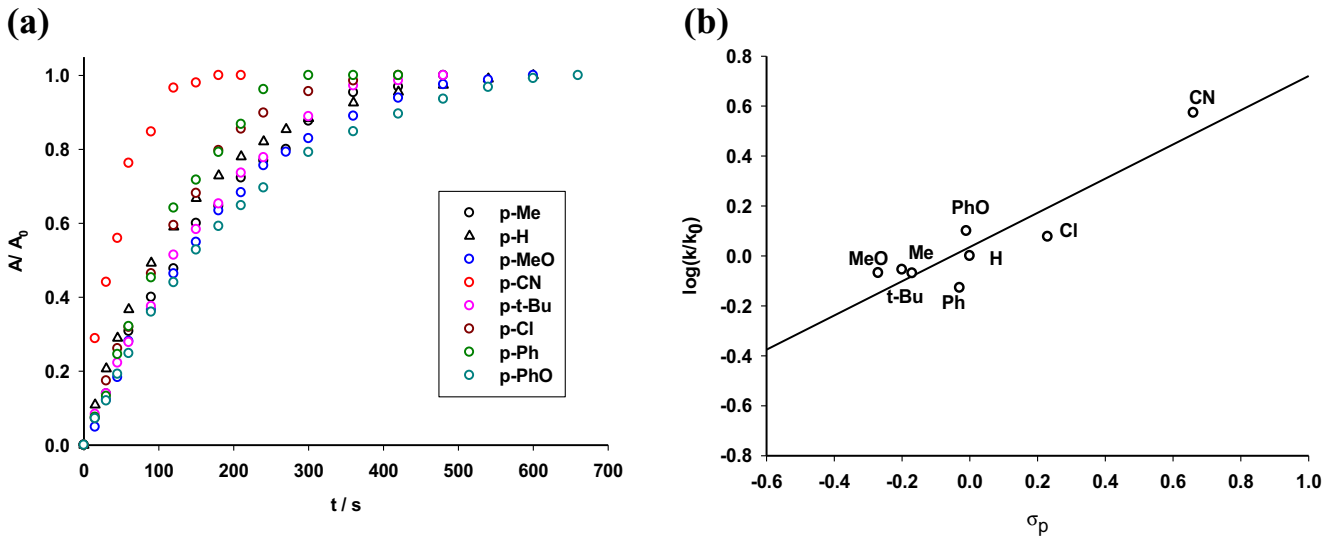

Figure 4. (a) Plots of grow-in of benzophenones derivatives in CTAC (0.020 M) solution. (b) Hammett Correlation of the log (k/k_0) with the σ_p substituent parameters for the irradiation of aryl benzoates in CTAC (0.020 M) solution.

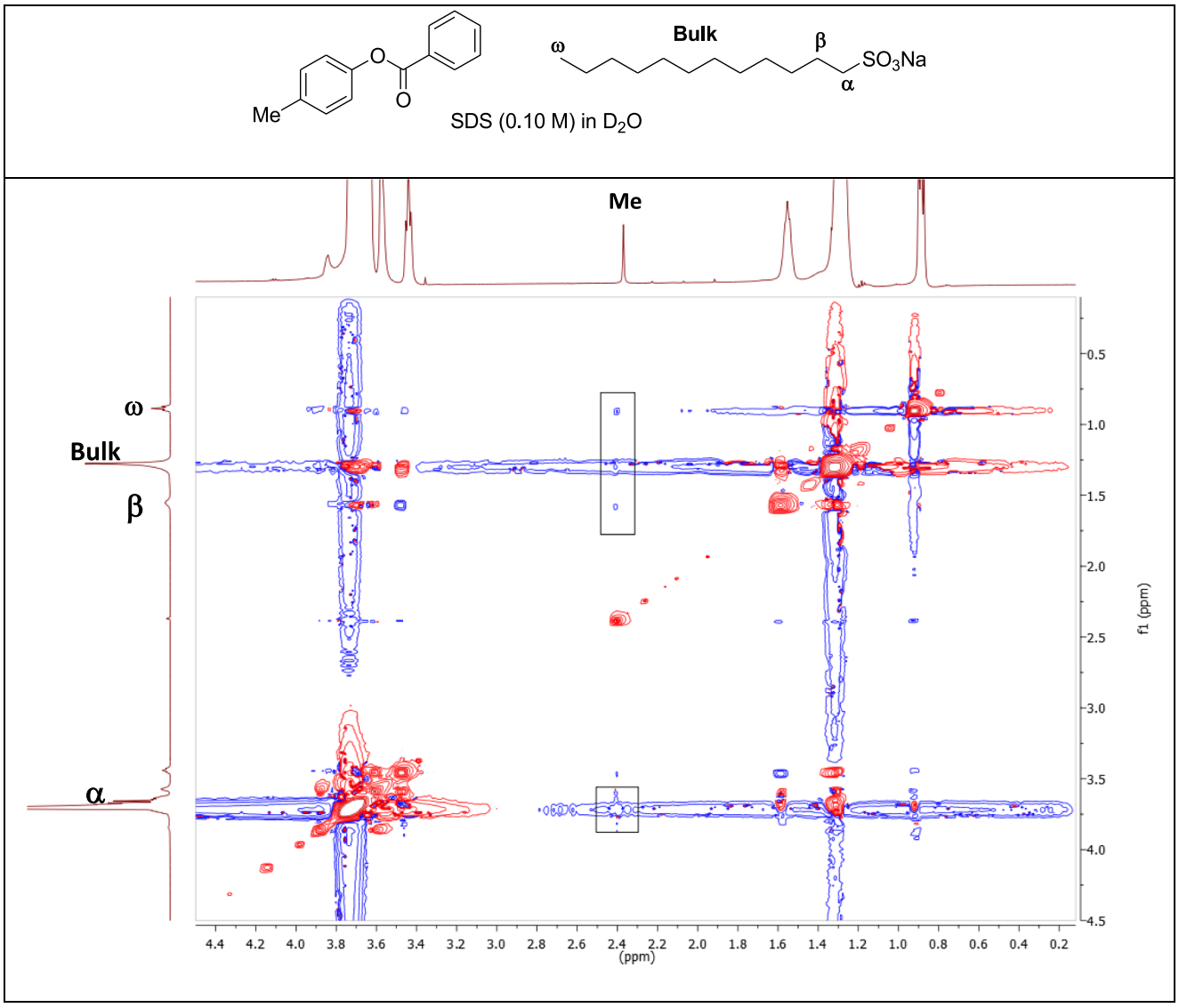

Figure 5. 2D NOESY contour plot of a solution of SDS (0.10 M) and benzoate **3** (5 mM) in D_2O at room temperature.

to measure the binding constants, respectively. The NOESY experiments have been often employed to determine the extent of coaggregation between two different kinds of surfactants in water and also to estimate qualitatively the localization of substrates inside the micelle (29,34). Indeed, the presence of cross-peaks between the diagnostic signals of the substrate and the surfactants in the contour plots indicates such interaction to occur (29,34). In Fig. 5 is shown the contour plot obtained after a NOESY experiment that was performed for p-methylphenyl benzoate **3** (5 mM) in a solution of SDS (0.10 M) in D_2O at room temperature. The protons of the surfactant SDS and those of methyl group of benzoate **3** are also highlighted in the same figure. The black framed insets underline the NOE (nuclear Overhauser effect) between the signals belonging to the α, β, ω and the bulk protons of the surfactant SDS and the methyl protons of p-methylphenyl benzoate **3** confirming the location of the benzoate within the hydrophobic core. NOESY experiments have been also carried out for benzoate **1** in solutions of SDS and Brij-P35 in D_2O and for benzoate **9** in solution of SDS in D_2O (see Figures S7–S9). Cross-peaks of diagnostic signals were observed in the 2D NMR contour plots also in these cases. However, all the NOESY experiments performed with benzoates **1**, **3**

Table 3. Binding constants (K_b) in water of surfactants (SDS, Brij-P35 and CTAC) and aryl benzoates.

	K_b/M^{-1}		
Aryl benzoates; R	SDS*	Brij-P35*	CTAC
1; OMe	1402	1398	70
2; OPh	80	581	31
3; Me	127	69	24
4; t-Bu	539	423	26
5; H	42	63	16
6; Ph	10	26	22
7; Cl	10	162	33
8; COOEt	102	1774	157
9; CN	18	1394	41
10; NO_2	74	181	32

*Data taken from Reference (34) except for compounds **7** and **8**.

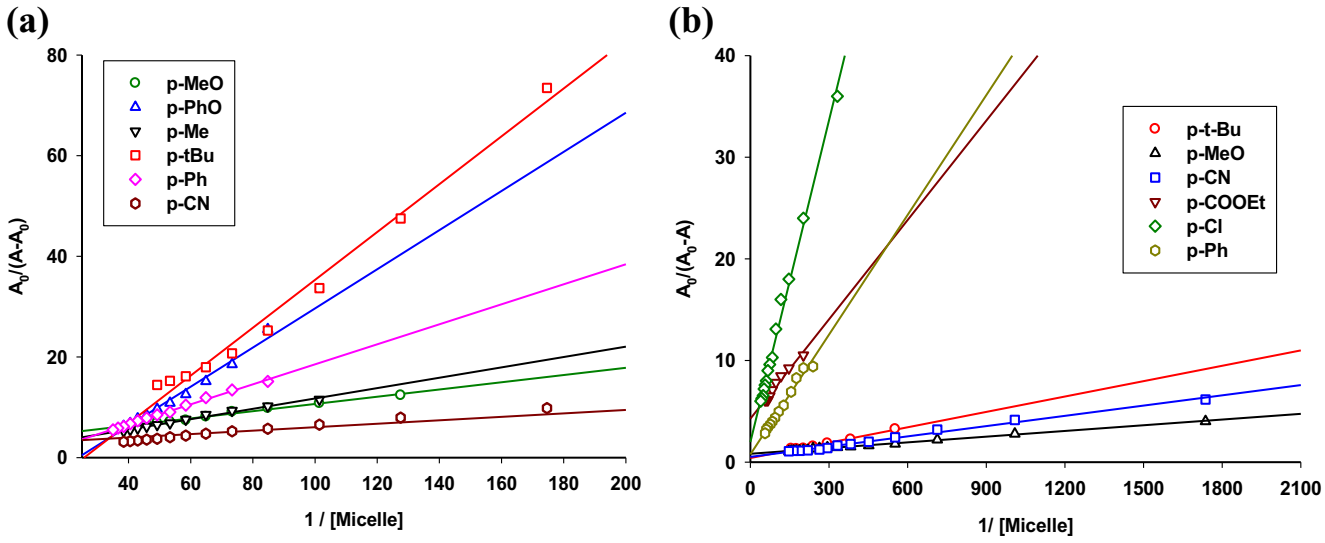

Figure 6. Plots of reciprocal of $(A_0/(A-A_0)$ vs reciprocal of concentration of surfactants in water at room temperature: (a) CTAC and (b) SDS.

Table 4. Energy (*E*) of the lowest allowed transition obtained for the optimized geometries of the aryl benzoates (**1**–**10**) and 5-substituted-2-hydroxybenzophenone (**1a**–**10a**) in cyclohexane or methanol (SMD) at the TD-PBE0/6-311 + g(2d,p)//PW6B95D3/def2-SVP and TD-CAM-B3LYP/6-311 + g(2d,p)//PW6B95D3/def2-SVP

	Cyclohexane		Methanol	
	E (PBE0) (eV)	*E*(CAM-B3LYP) (eV)	*E* (PBE0) (eV)	*E*(CAM-B3LYP) (eV)
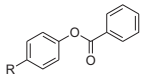				
OMe (**1**)	4.08	4.94	4.13	4.99
OPh (**2**)	4.12	4.90	4.22	4.95
Me (**3**)	4.43	5.08	4.51	5.07
t-Bu (**4**)	4.44	5.08	4.52	5.07
H (**5**)	4.66	5.07	4.76	5.06
Ph (**6**)	4.17	4.77	4.26	4.83
Cl (**7**)	4.52	5.06	4.61	5.05
COOEt (**8**)	4.69	5.04	4.78	5.03
CN (**9**)	4.73	5.02	4.79	5.02
NO_2 (**10**)	4.03	4.10	4.04	4.11
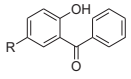				
OMe (**1a**)	3.27	3.57	3.26	3.58
OPh (**2a**)	3.39	3.77	3.26	3.67
Me (**3a**)	3.59	3.87	3.59	3.88
t-Bu (**4a**)	3.56	3.88	3.62	3.93
H (**5a**)	3.74	4.03	3.74	4.06
Ph (**6a**)	3.39	3.78	3.36	3.78
Cl (**7a**)	3.54	3.88	3.54	3.92
COOEt (**8a**)	3.82	4.12	3.83	4.15
CN (**9a**)	3.78	4.11	3.77	4.16
NO_2 (**10a**)	3.89	4.14	3.89	4.16

and **9** demonstrate that it is challenging to estimate precisely the location of the aryl benzoates with accuracy but we can suggest that the aryl benzoates are located within the hydrophobic core of the micelle because the proton nuclei of the benzoates correlate nicely with the proton nuclei of the surfactants as can be seen through the cross-peaks of the contour plots.

Next, we have focused in the measurement of the binding constants K_b between the surfactants and the aryl benzoates using UV-visible spectroscopy applying the methodology reported earlier in the literature for the case of aryl acetamide (29). A linear relationship is observed between $(A–A_0)^{-1}$ and the reciprocal of the concentration of the surfactant according to equation 3 where A and A_0 are the absorbance at the maxima wavelength in the presence and absence of surfactant, respectively, and ϵ_S and ϵ_C are the molar absorptivity of the aryl benzoates and the complex.

$$\frac{A_0}{(A-A_0)} = \frac{\varepsilon_S}{\varepsilon_C} + \frac{\varepsilon_S}{\varepsilon_C \cdot K_b}\frac{1}{[\text{Surf}]} \quad (3)$$

The ratio between the intercept and the slope of the linear relationship provides the binding constants (K_b) of the aryl benzoates which are collected in Table 3. On the other hand, Fig. 6 shows the experimental data and the best linear regression curves obtained for some aryl benzoates and surfactants such as CTAC and SDS, respectively. The plots for the other system (Brij-P35 as the surfactant) are collected in Figure S6.

The data collected in Table 3 show that the benzoates bind to the micelles but it is apparent that the K_b values obtained in Brij-P35 were found to be higher than those obtained in SDS and CTAC. An estimation of a minimum value around 190 M for the binding constant (K_b) of Brij-P35 surfactant have been also reported (17). The behavior observed between Brij-P35 and the benzoates can be ascribed to a more nonpolar environment of the micelle core which was previously measured using pyrene as a micropolarity probe (45). Indeed, benzoates possessing hydrophobic character such as **1**, **2**, **4**, **8** and **9** in Brij-P35 micellar solution, show high K_b values. Generally, the binding constants (K_b) obtained for aryl benzoates **1**–**10** are typical of aromatic solutes as it was previously reported in the literature (46–49). In fact, substrates like benzonitrile, methyl and ethyl benzoates, acetanilide and benzamide among others show binding constants ranging between 8 to 100 M (47). Furthermore, it

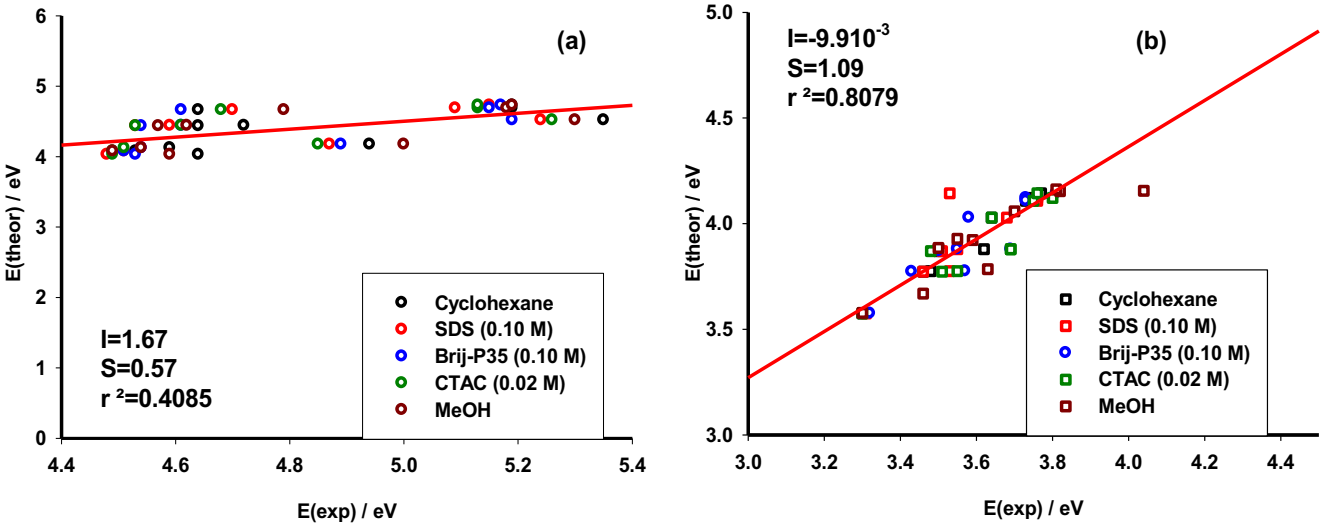

Figure 7. Correlation of the theoretical and experimental energies of the lower absorption band of: (a) *p*-substituted phenyl benzoates and (b) 5-substituted-2-hydroxybenzophenones.

was found for a series of substituted benzoyl chloride that the binding constants in SDS and in CTAC are in the same order of magnitude (50), and this trend is observed for our experimental data with the exception of benzoates **1** and **4**.

Finally, NOESY experiments demonstrated that aryl benzoates are located within the hydrophobic core of the micelle because cross-peaks between proton nuclei of the benzoates correlate nicely with the proton nuclei of the surfactants as can be seen in the contour plots. Furthermore, it was found that aryl benzoates **1**-**10** bind efficiently to the SDS, CTAC and Brij-P35 micelles, respectively, as can be judge from the binding constants (K_b) which are typical constants observed for aromatic compounds measured using UV-visible spectroscopy. Both spectroscopic methods confirm and reinforce the idea that the photochemical reaction takes place within the hydrophobic core of the ionic and nonionic micelles which can be considered like mini-photochemical reactors.

We also computed the UV-Vis spectra of the species involved in the study using two different functionals, namely PBE0 and CAM-B3LYP. Both functionals afforded similar results. Interestingly, the computed spectra followed more closely the experimental values for the benzophenones, while the aryl benzoates were not affected by the substitution (see Table 4). However, a nice fit could be plotted comparing the theoretical and experimental values using the PBE0 functional for aryl benzoates whereas CAM-B3LYP functional was used for substituted benzophenones, as depicted in Fig. 7.

CONCLUSION

The photo-Fries rearrangement reaction of aryl benzoates examined in this paper takes place efficiently in cyclohexane and with noticeable selectivity in micellar media. Indeed, high selectivity was observed in favor of the formation of 5-substituted-2-hydroxybenzophenone derivatives in micellar media using ionic (SDS and CTAC) and neutral (Brij-P35) surfactants. These benzophenone derivatives were obtained in yields up to 95 % while no substituted phenols were detected. The substituent effect was also studied on the UV-visible absorption spectroscopy and on the photoreaction. No significant effect of the solvent on the low absorption band energy (*E*) values of aryl benzoates and 2-hydoxybenzophenone derivatives was observed when moving from cyclohexane to polarity brought the hydrophobic core of the micelles. However, a noticeable substituent effect was observed on the energy (*E*) values of both the aryl benzoates and benzophenone derivatives displaying a hypsochromic shift after quantification by means of the Hammett linear free energy relationships (LFER). The substituent effect was also analyzed on the photoreaction of aryl benzoates, and a low role of the substituents on the homolytic fragmentation of the C-O bond of the ester group was observed in cyclohexane and micellar solutions. In fact, the ρ values indicated that electron-withdrawing substituents accelerate the photoreaction while electron-donor substituents deaccelerate the photoreaction.

The nature of surfactants has also displayed a noticeable effect on the photoreaction, and it was found that the photoreaction performed in CTAC solution is significantly lower than in SDS or Brij-P35 solutions. This behavior was attributed to the chloride anion of CTAC surfactant because it operates like an external heavy atom quencher quenching the singlet excited state of the aryl benzoate and promoting the deactivation through a competitive intersystem crossing pathway.

Location of the aryl benzoates with 2D NOESY NMR spectroscopy in the shell or in the hydrophobic core of the micelle and measurement of the binding constants (K_b) between the benzoates and the surfactants account for the selective behavior observed where diffusion of the radical species from the micelle is inhibited. On the other hand, benzophenone derivatives, as the main photoproducts, and the p-substituted phenols were formed when the irradiations were carried out in cyclohexane but no selectivity was observed.

The calculated spectra were used to compare the theoretical UV-Vis values with the experimental ones, showing the same trend observed.

Finally, the finding that the selectivity observed in the photo-Fries rearrangement of some aryl benzoates in green and sustainable micellar media gives 5-substituted-2-hydroxybenzophenone derivatives in yields up to 95 % could be applied in the

preparation of a new wide variety of substituted-2-hydroxybenzophenone derivatives and the results will be independent from the nature of the surfactant employed to perform the photoreactions.

Acknowledgements—SMB is research member of CONICET, Argentina.

SUPPORTING INFORMATION

Additional supporting information may be found online in the Supporting Information section at the end of the article:

Appendix S1. Additional supporting information may be found online in the Supporting Information section at the end of the article

Data S1. Time-resolved UV-visible absorption spectroscopy under steady-state.

Data S2. Relative absorption (A/A0) versus time in homogeneous and heterogeneous media.

Data S3. Measure of the aryl benzoate consumption rate constants (k).

Data S4. Hammett Linear correlations.

Data S5. Determination of the binding constants Kb in micellar media.

Data S6. 2D NMR (NOESY Experiments) spectra in micellar media.

Data S7. Physical and spectroscopic characterization of compounds 7, 7a, 8 and 8a.

Data S8. References.

Data S9. Copy of the 1H and 13C spectra of aryl benzoates 7 and 8.

Data S10. Copy of the 1H and 13C spectra of 2-hydroxy-5-substituted benzophenones 7a and 8a.

Data S11. Cartesian Coordinates.

REFERENCES

1. Tung, C. H., L. Z. Wu, L. P. Zhang and B. Cheng (2003) Supramolecular systems as microreactors: Control of product selectivity in organic phototransformation. *Acc. Chem. Res.* **36**, 39–47.
2. Liu, R. S. H. and G. S. Hammond (2005) Reflection on medium effects on photochemical reactivity. *Acc. Chem. Res.* **38**, 396–403.
3. Miranda, M. A. and F. Galindo (2003) The Photo-Fries rearrangement. *Photochemistry of Organic Molecules in Isotropic and Anisotropic Media* (Edited by V. Ramamurthy and K. S. Schanze) Chapter 2. Marcel Dekker, New York. 43–131.
4. Natarajan, A., L. S. Kaanumale and V. Ramamurthy (2004) Manipulating Photochemical Reactions. *CRC Handbook of Organic Photochemistry and Photobiology*, Vol. 3 (Edited by W. Horspool and F. Lenci), pp. 107–147.CRC Press, Boca Raton, FL.
5. Turro, N. J. (2000) From boiling stones to smart crystals: Supramolecular and magnetic isotope control of radical−radical reactions in zeolites. *Acc. Chem. Res.* **33**, 637–646.
6. Ramamurthy, V. (2000) Controlling photochemical reactions via confinement: zeolites. *J. Photochem. Photobiol. C: Photochemistry Reviews* **1**, 145–166.
7. Fendler, J. H. and E. J. Fendler (1975) *Catalysis in Micellar and Macromolecular Systems*. Academic Press, London, UK.
8. Holland, P. M. and D. N. Rubingh (1992) Mixed Surfactant System, An Overview. *Mixed Surfactant System* (Edited by P. M. Holland and D. N. Rubingh), pp. 2–30. American Chemical Society. Washington, DC.
9. Gu, W. and R. G. Weiss (2001) Extracting fundamental photochemical and photophysical information from photorearrangements of aryl phenylacylates and aryl benzyl ethers in media comprised of polyolefinic films. *J. Photochem. Photobiol. C: Photochemistry Reviews* **2**, 117–137.
10. Kaanumalle, L. S., C. L. D. Gibb, B. C. Gibb and V. Ramamurthy (2007) Photo-Fries reaction in water made selective with a capsule. *Org. Biomol. Chem.* **5**, 236–238.
11. Kulasekharan, R., R. Choudhurry, R. Prabhakar and V. Ramamurthy (2011) Restricted rotation due to the lack of free space within a capsule translates into product selectivity: Photochemistry of cyclohexyl phenyl ketones within a water-soluble organic capsule. *Chem. Commun.* **47**, 2841–2843.
12. Kaanumalle, L. S., J. Nithyanandhan, M. Pattabiaman, N. Jayaraman and V. Ramamurthy (2004) Water-soluble dendrimers as photochemical reaction media: Chemical behavior of singlet and triplet radical pairs inside dendritic reaction cavities. *J. Am. Chem. Soc.* **126**, 8999–9006.
13. Menger, F. M. (1979) The structure of micelles. *Acc. Chem. Res.* **12**, 111–117.
14. Turro, N. J. and J. Mattay (1981) Photochemistry of some deoxybenzoins in micellar solutions. Cage effects, isotope effects, and magnetic field effects. *J. Am. Chem. Soc.* **103**, 4200–4204.
15. Turro, N. J., G. Sidney Cox and M. A. Paczkowski (1985) Photochemistry in micelles. In *Topics in Current Chemistry, Photochemistry and Organic Synthesis* (Edited by F. L. Boschke). pp 57. Springer-Verlag, New York.
16. Kano, K. and T. Matsuo (1973) Photochemical reaction of the p-benzoquinones in micellar system. *Chem. Lett.* **2**, 1127–1132.
17. Kano, K., Y. Takada and T. Matsuo (1975) Photochemistry in micellar system. II. Photochemical reduction of b-arylquinonesulfonates in the presence of cationic surfactants. *Bull. Chem. Soc. Jp.* **48**, 3215–3219.
18. Yasudat, M., Y. Nishinaka, T. Nakazono, T. Hamasaaki, N. Nakamura, T. Shiragami, C. Pac and K. Shima (1998) Photochemistry of flavins in micelles: specific effects of anionic surfactants on the monomerization of thymine cyclobutane dimers photosensitized by tetra-O-acyl riboflavins. *Photochem. Photobiol.* **67**, 192–197.
19. Souza Santos, M., M. P. F. Morais Del Alma, A. S. Ito and R. M. Z. G. Naal (2014) Binding of chloroquine to ionic micelles: Effect of pH and micellar surface charge. *J. Lumin.* **147**, 49–58.
20. Anderson, J. C. and C. B. Reese (1960) *Photoinduced Fries Rearrangement*, p. 217. Proc. Chem. Soc, London.
21. Bellus, D. (1971) Photo-Fries rearrangement and related photochemical [1, j] – shift (j: 3, 5, 7) of carbonyl and sulfonyl groups. *Adv. Photochem.* **8**, 109–159.
22. Miranda, M. A. (1995) The Photo-Fries rearrangement. *CRC Handbook of Organic Photochemistry and Photobiology* (Edited by W. Horspool and P. S. Song) pp 570. CRC Press, Boca Raton, FL.
23. Singh, A. K. and T. S. Raghuraman (1985) Photorearrangement of phenyl cinnamates under micellar environment. *Tetrahedron Lett.* **26**, 4125–4128.
24. Yie, R. Q., Y. C. Liu and X. G. Lei (1992) The photo-Fries rearrangement of α-naphthyl acetate in cyclodextrin and micelle. *Res. Chem. Intermed.* **18**, 61–69.
25. Chenevert, K. and N. Voyer (1984) Photochemical rearrangement of phenyl benzoate in the presence of cyclodextris and amylose. *Tetrahedron Lett.* **25**, 5007–5008.
26. Singh, A. K. and T. S. Raghuraman (1986) Photobehavior of N-aryl amides in micelle. *Synth. Commun.* **16**, 485–490.
27. Iguchi, D., R. Erra-Balsells and S. M. Bonesi (2016) Photo-Fries rearrangement of aryl acetamides: Regioselectivity induced by the aqueous micellar green environment. *Photochem. Photobiol. Sci.* **15**, 105–116.
28. Syamala, M. S., B. Nageswer Rao and V. Ramamurthy (1998) Modification of photochemical reactivity by cyclodextrin complexation: product selectivity in the photo-Fries rearrangement. *Tetrahedron* **44**, 7234–7242.
29. Nasetta, M., R. H. De Rossi and J. J. Cosa (1988) Influence of cyclodextrins on the photo-Fries rearrangement of acetanilide. *Can. J. Chem.* **66**, 2794–2798.
30. Morohoshi, K., H. Yamamoto, R. Kamata, F. Shiraishi, T. Koda and M. Morita (2005) Estrogenic activity of 37 components of commercial sunscreen lotions evaluated by in vitro assays. *Toxicol. In Vitro* **19**, 457–469.
31. Venu, T. D., S. Shashikauth, S. A. Khanun, S. Naveen, A. Firdouse, M. A. Sridhar and J. Shashidhara Prasad (2007) Synthesis and

crystallographic analysis of benzophenone derivatives. The potential anti-inflammatory agents. *Bioorg. Med. Chem.* **15**, 3505–3514.
32. Coronado, M., H. De Haro, X. Deng, M. A. Rempel, R. Lavado and D. Schlenck (2008) Estrogenic activity and reproductive effects of the UV-filter oxybenzone (2-hydroxy-4-methoxyphenyl-methanone) in fish. *Aquatic Tox.* **90**, 182–187.
33. Maciel Rezende, C. M., L. de Almeida, E. D. Costa, F. Robeiro Pires, K. Ferreira Alves, C. Viegas Junior, D. Ferreira Dias, A. C. Dominguetto, M. J. Marques and M. H. Dos Santos (2013) Synthesis and biological evaluation against *Leishmania amazonensis* of a series of alkyl-substituted benzophenones. *Bioorg. Med. Chem.* **21**, 3114–3119.
34. Siano, G., S. Crespi, M. Mella and S. M. Bonesi (2019) Selectivity in the photo-Fries rearrangement of some aryl benzoates in green and sustainable media. Preparative and mechanistic studies. *J. Org. Chem.* **84**, 4338–4352.
35. Pracht, P., F. Bohle and S. Grimme (2020) Automated exploration of the low-energy chemical space with fast quantum chemical methods. *Phys. Chem. Chem. Phys.* **22**, 7169–7192.
36. Frisch, M. J., G. W. Trucks, H. B. Schlegel, G. E. Scuseria, M. A. Robb, J. R. Cheeseman, G. Scalmani, V. Barone, G. A. Petersson, H. Nakatsuji, X. Li, M. Caricato, A. V. Marenich, J. Bloino, B. G. Janesko, R. Gomperts, B. Mennucci, H. P. Hratchian, J. V. Ortiz, A. F. Izmaylov, J. L. Sonnenberg, D. Williams-Young, F. Ding, F. Lipparini, F. Egidi, J. Goings, B. Peng, A. Petrone, T. Henderson, D. Ranasinghe, V. G. Zakrzewski, J. Gao, N. Rega, G. Zheng, W. Liang, M. Hada, M. Ehara, K. Toyota, R. Fukuda, J. Hasegawa, M. Ishida, T. Nakajima, Y. Honda, O. Kitao, H. Nakai, T. Vreven, K. Throssell, J. A. Jr Montgomery, J. E. Peralta, F. Ogliaro, M. J. Bearpark, J. J. Heyd, E. N. Brothers, K. N. Kudin, V. N. Staroverov, T. A. Keith, R. Kobayashi, J. Normand, K. Raghavachari, A. P. Rendell, J. C. Burant, S. S. Iyengar, J. Tomasi, M. Cossi, J. M. Millam, M. Klene, C. Adamo, R. Cammi, J. W. Ochterski, R. L. Martin, K. Morokuma, O. Farkas, J. B. Foresman and D. J. Fox (2016). *Gaussian 16, Revision B.01*. Gaussian, Inc., Wallingford, CT.
37. Goldstein, S. and J. Rabani (2008) The ferrioxalate and iodide-iodate actinometers in the UV region. *J. Photochem. Photobiol., A:Chem.* **193**, 50–55.
38. Turro, N. J. (1978) *Modern Molecular Photochemistry*. Benjamin/Cummings, Menlo Park, CA.
39. Turro, N. J., V. Ramamurthy and J. C. Scaiano (2010) *Modern Molecular Photochemistry of Organic Molecules*. University Science Books, Sausalito, CA.
40. Bonesi, S. M., M. Mesaros, F. M. Cabrerizo, M. A. Ponce, G. Bilmes and R. Erra Balsells (2007) The photophysics of nitrocarbazoles used as UV-MALDI matrices: Comparative spectroscopic and optoacoustic studies of mononitro- and dinitrocarbazoles. *Chem. Phys. Lett.* **446**, 49–55.
41. Cors, A., S. M. Bonesi and R. Erra Balsells (2008) Photoreduction of nitro arenes by formic acid in acetonitrile at room temperature. *Tetrahedron Lett.* **49**, 1555–1558.
42. Hammett, L. P. (1935) Some relations between reaction rates and equilibrium constants. *Chem. Rev.* **17**, 125–136.
43. Ewing, D. F. (1978) Correlation of NMR chemical shifts with Hammett σ values and analogous parameters. *Correlation Analysis in Chemistry: Recent Advances* (Edited by N. B. Chapman and J. Shorter). Plenum Press, New York, NY, 357–396.
44. Hansch, C., A. Leo and R. W. Taft (1991) A survey of Hammett substituent constants and resonance and field parameters. *Chem. Rev.* **91**, 165–195.
45. Campos Rey, P., C. Cabaleiro Lago and P. Hervés (2010) Solvolysis of substituted benzoyl chlorides in nonionic and mixed micellar solutions. *J. Phys. Chem. B* **114**, 14004–14011.
46. Sepulveda, L., E. Lissi and F. H. Quina (1986) Interactions of neutral molecules with ionic micelles. *Adv. Colloid Interface Sci.* **25**, 1–57.
47. Quina, F. H. and E. O. Alonso (1995) Incorporation of nonionic solutes into aqueous micelles: A linear solvation free energy relationship analysis. *J. Phys. Chem.* **99**, 11708–11714.
48. Abraham, H., H. S. Chadha, J. P. Dixon, C. Rafols and C. Treiner (1995) Hydrogen bonding Part 40. Factors that influence the distribution of solutes between water and sodium dodecylsulfate micelles. *J. Chem. Soc. Perkin Trans*. **2**, 887–894.
49. Abraham, H., H. S. Chadha, J. P. Dixon, C. Rafols and C. Treiner (1997) Hydrogen bonding. Part 41.1 Factors that influence the distribution of solutes between water and hexadecylpyridinium chloride micelles. *J. Chem. Soc. Perkin Trans.* **2**, 19–24.
50. Bunton, C. A., N. D. Gillitt, M. M. Mhala, J. R. Moffat and A. K. Yatsimirsky (2000) Micellar charge effects upon hydrolysis of substituted benzoyl chlorides. Their relation to mechanism. *Langmuir* **16**, 8595–8603.